Full length article

Laminated beams/shafts of annular cross-section subject to combined loading

Shuguang Li [a], Michael S. Johnson [a,*], Elena Sitnikova [a], Richard Evans [b], Preetum J. Mistry [a]

[a] *Composites Research Group, Faculty of Engineering, University of Nottingham, Advanced Manufacturing Building, Jubilee Campus, Nottingham, NG8 1BB, UK*
[b] *Gas Turbine and Transmission Research Centre (G2TRC), University of Nottingham, Nottingham, NG7 2TU, UK*

ARTICLE INFO

ABSTRACT

A novel stress analysis method is developed for the efficient design of radially laminated annular beams/shafts subject to arbitrary load combinations. The analysis is conducted using classic laminate theory (CLT) in conjunction with a mechanics of materials (MoM) approach based on the plane section assumption. Global loads are related to the global deformations and are expressed in terms of the generalised laminate strains in CLT. The analysis is verified against MoM for a homogeneous and isotropic tube. Further validation against the finite element method is shown for general cases in terms of loading and laminate layups with almost perfect agreement.

1. Introduction

Fibre reinforced polymer composites are used extensively as laminated panels, typically in the transportation sector where benefits arise from structural lightweighting. Carbon fibre reinforced polymers (CFRP) are the preferred material having a high specific strength and stiffness. The analysis of components made of CFRP is well established with classic laminate theory (CLT) [1] typically being employed. When laminated CFRP components form complex structures subjected to combined loading, the finite element method (FEM) is utilised as an effective problem solver. However, any finite element analysis (FEA) requires the availability of a commercial software and an engineer with a strong FEM background. Balanced judgements on element type selection, appropriate meshing with its convergence checked, load application techniques and representative boundary conditions are required. This is a non-trivial exercise in respect of time and cost, particularly when design iterations are required for an optimum solution.

Prior to FEA, an efficient design tool is needed to specify the initial layup of the laminated composite based on sufficiently simple analysis, namely CLT. In this paper, such a tool is presented for designing lightweight rotating axles and shafts to transmit torques. These are used widely in automotive and aerospace power trains, for example, as driven wheel and helicopter tail rotor drive shafts, respectively. These components often are subjected to other loads such as pulling or pushing, internal pressure, bending and transverse shear forces. Such applications include aerospace gearbox lay shafts, wind turbine main shafts and railway axles which demand the shaft to withstand fully

reversed bending under heavy loading to high rotating cycles. The shafts are usually hollow, forming an annular cross-section, to enhance lightweighting. Use of oriented CFRP offers low density, high strength and desirable fatigue properties [2].

Specific to the efficient design tool, the aim of this paper is to establish a CLT based analytical formulation for calculating the ply stresses under combined loading, which can be further employed to predict ply failure, within the wall of a radially laminated shaft of annular cross-section.

2. Background

The stress analysis of coaxial orthotropic tubes typically is founded on the Lekhnitskii formalism [3] which equilibrates stress functions and strain compatibility equations to form a system of partial differential equations. The tube stresses are obtained from the stress functions using those partial differential equations. Jolicoeur and Cardou [4] extended Lekhnitskii's work on a single cylinder by providing a solution for the general case of coaxial orthotropic cylinders. Their elasticity solution was accurate for specific problems, but its application would be cumbersome for multi-layered problems. Another popular approach was described by Stroh [5], where use was made of compatible displacement and equilibrium equations to form a system of partial differential equations. Displacements are then obtained from them. The Lekhnitskii and Stroh approaches, when applied to multiple layers, generate a large system of equations to be solved (stress or displacement, respectively). The resulting mathematical complexity hinders practical implementation of these techniques.

---

* Corresponding author.
  E-mail address: Michael.Johnson@nottingham.ac.uk (M.S. Johnson).

Shadmehri et al. [6] used non-classical laminate theory to determine the equivalent flexural stiffness for the composite. The approach yields two independent loading scenarios: (1) extension and twisting of the tube and (2) bending and transverse shear within the tube. Relatively, the approach followed in this work is closest to that presented in this paper, with the scope systematically and substantially broadened so that it is not restricted to any specific layup as was assumed by those authors. Nevertheless, validation against the method by Shadmehri et al. would have been beneficial. However, the results extracted from that manuscript for the bending stiffness seemed to be an order of magnitude higher than what one would expect according to mechanics of materials (MoM) solution with all fibres aligned along the axis of the beam and hence the highest bending rigidity one could possibly obtain. As a result, an attempt to cross validate the present analysis with that work was not possible.

Silvestre [7] developed a Generalised Beam Theory (GBT) formulation to analyse the linear behaviour of circular hollow section (CHS) members. As the method essentially was shell theory based, it had the ability to predict the deformation of the cross-section. However, the approach became manageable only after restrictions, such as vanishing membrane shear strains in the transverse direction. The analysis also was non-trivial to implement, requiring an appropriate numerical method, such as FEM, finite difference, or similar to support it.

High-order theories have been presented more recently offering elegant solutions for the analysis of beams with circular cross sections [8] as well as curved, laminated beams [9]. The current problem of a laminated tube of annular cross section likely would benefit from these approaches. However, given the current lack of a solution to the problem, even with CLT, a basic approach is desirable before escalating to a high-order theory as a future development.

In the present paper, the problem of tubes of a radially laminated annular cross-section under combined loading as specified in the Introduction (Section 1) will be addressed. Segments along the circumference of the cross-section are considered as a conventional laminate governed by CLT. The generalised strains in the segment will be related to the global deformation of the tube following simple kinematics based on the plane section assumption. The generalised stresses over the segment can be related to the global loads after appropriate integration of the stresses along the complete circumference of the cross-section. This leads to the simplest and conceptually most straightforward approach amongst those reviewed above, and yet is the most comprehensive in terms of loading conditions and laminate layup. Assisted with a material failure criterion, the analysis would offer an efficient and effective means for a designer to optimise laminated tubular structures after identification of the critical cross-sections.

3. Foundations to the analytical formulation

Prior to the development of the tubular analysis (Section 4), the underlying foundations are established in the following subsections.

3.1. Description of coordinate systems and tube parameters

Three, right-handed coordinate systems are involved for the analysis as shown in Fig. 1.

(1) Global Cartesian coordinate system, X–Y–Z. Loads and corresponding deformations of the tube are presented in this coordinate system.
(2) Laminate cylindrical coordinate system, ξ-η-ζ. The concentric annular tube layers, also termed plies or laminae, making up the laminate structure are subjected to generalised stresses and strains described within this coordinate system according to CLT. Specifically, the axial direction, ξ, is oriented parallel to the global X axis.
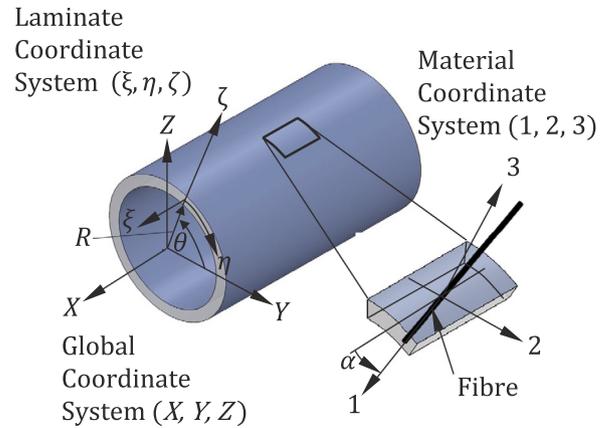
Fig. 1. Definition of the right handed global X–Y–Z, laminate ξ-η-ζ and material 1–2–3 coordinate systems.
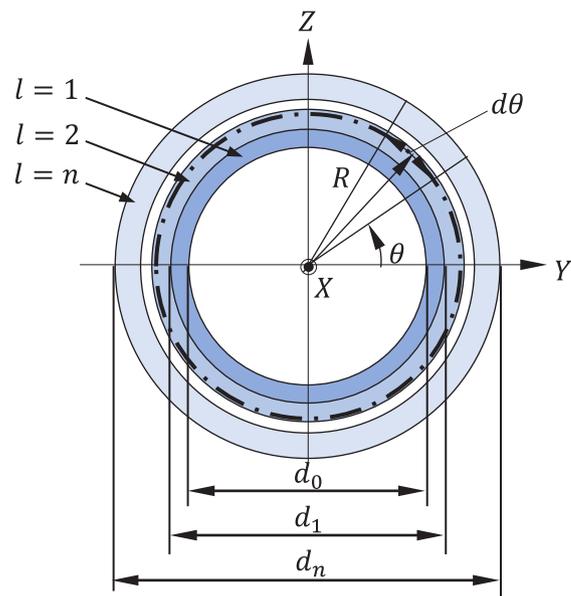
Fig. 2. A cross-section through a laminated annular tube consisting of n layers.

(3) Material local coordinate system 1–2–3. Each laminate is made up of a stack of plies with mechanical properties defined in terms of this local or principal coordinate system of the material. Apparently, axis 3 coincides with axis ζ.

A cross-section through a series of concentric annular tube layers in the global Y-Z plane is shown in Fig. 2 in generalised form. The consecutive annular layers, $l = 1, 2, \ldots n$, have increasing inner diameters. To define the geometry of the cross-section, the diameters of the $n+1$ interfaces, including the inner and outer surfaces, are used. These are denoted as d_0, $d_1 \ldots d_n$. The radius, R, is taken at the midsurface of the tube wall. Angular position is indicated by θ, with incremental changes in position denoted as $d\theta$ and is related to the arc length on the reference surface as $ds = Rd\theta$.

3.2. Global loads applied to the tube

The loads the tube is capable of sustaining are illustrated in Fig. 3. These loads are conventionally dealt with in mechanics of materials (MoM) [10] from which sign conventions will be adapted in conjunction with those from the CLT [1]. For the ease of analysis, they are
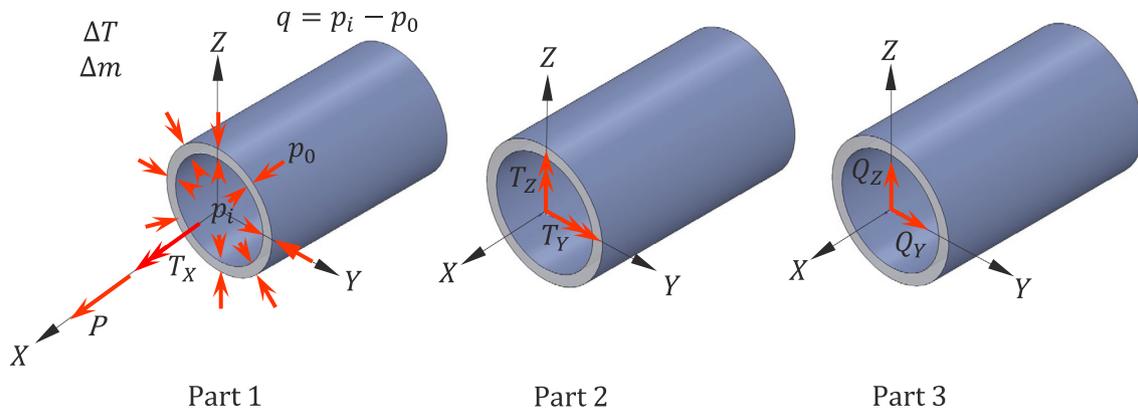
Fig. 3. Resultant forces and moments acting on the tube cross-section and referenced to the global coordinate system, X–Y–Z. Hygrothermal effects (ΔT and Δm) are considered within Part 1.

separated into three parts and the superposition law will be used to obtain the combined effects, given the linear nature of the problem.

Part 1:

- The difference between the internal pressure, p_i, and external pressure, p_o, applied uniformly to the walls of the laminated tube and denoted as q(N/m^2), outward direction as positive.
- Axial force, indicated as P (N), aligned with the global tube axis, X.
- Torque about the global X axis and indicated as T_X (N m).
- Temperature change ΔT which could be due to the change in working environment relative to the ambient temperature, or the cured stress-free state during the curing process of the composite.
- Moisture absorption Δm which could be due to the change in working environment relative to the ambient state.

Part 2:

Bending moments about the global Y and global Z axes, shown as T_Y (N m) and T_Z (N m), respectively.

Part 3:

Shear forces along the global Y and Z axes, represented as Q_Y (N) and Q_Z (N), respectively.

3.3. Global deformations of the tube

Under the global loads described in Section 3.2, there are five global deformations: axial extension ε_X, angle of twist per unit length about the X, ϕ_X, rotations of the tube cross-section per unit length about the horizontal axis Y and vertical axis Z, ϕ_Y and ϕ_Z, respectively as well as an increase in radius, ρ, which is related directly to circumferential extension. Due to the anisotropy of the material and the layered construction, intricate coupling occurs. The partition of the load cases above will at least prevent direct coupling between load cases so that they can be analysed individually before being superposed to give a complete solution. The first objective of the analysis is to obtain the laminate generalised strains under each load case. They can then be superposed according to the superposition law to give the total laminate generalised strains.

The shear forces on the tubular beam cross-section, Q_Y and Q_Z, do not have a global deformation directly associated with them, due to the limitation of Bernoulli beam theory adopted. The effect of the shear forces is incorporated as a distributed membrane shear force as introduced in CLT within the analysis (Section 4.3). The laminate generalised strains from this load case can be obtained from the membrane shear force along the circumference of the tube.

The plane section assumption underlies the present analysis. This states that the cross-section of the tube remains plane and normal to the deformed tube axis, X, after deformation. As with all shaft design, identification of the locations of the critical cross-sections is necessary. Typically these are positions where the bending moment is large, where stress concentrations exist [11], sometimes in presence of a torque and/or other types of load.

3.4. Key relationships from the classic laminate theory (CLT)

The present analysis will be based on the concepts of conventional MoM to describe the global deformation of the tube, namely a bar for axial load, a shaft for torsion, a beam for transverse bending moments and shear forces, a cylindrical shell for internal pressure. The classic laminate theory (CLT) [1] is employed to account for the local deformation through the wall thickness of the tube. As a part of the Love–Kirchhoff hypothesis which underlies CLT, strains in a laminate $\{\varepsilon\}$ are linearly distributed over its thickness, that is, in the radial direction of the tube,

$$\{\varepsilon\} = \{\varepsilon^0\} + \zeta\{\kappa\} \tag{1}$$

where $\{\varepsilon^0\}$, or ε_ξ^0, ε_η^0, $\gamma_{\xi\eta}^0$, are membrane strains, $\{\kappa\}$, or κ_ξ, κ_η, $\chi_{\xi\eta}$, changes in curvature and ζ is the laminate coordinate through the thickness of the tube, outward as its positive direction. Together, $\{\varepsilon^0\}$ and $\{\kappa\}$ conventionally are referred to as the laminate generalised strains.

The generalised strains are related to the generalised stresses through the generalised stress–strain relationship defined in CLT as follows.

$$\begin{Bmatrix} \widehat{N}_\xi \\ \widehat{N}_\eta \\ \widehat{N}_{\xi\eta} \\ \widehat{M}_\xi \\ \widehat{M}_\eta \\ \widehat{M}_{\xi\eta} \end{Bmatrix} = \begin{bmatrix} A_{11} & A_{12} & A_{16} & B_{11} & B_{12} & B_{16} \\ A_{12} & A_{22} & A_{26} & B_{12} & B_{22} & B_{26} \\ A_{16} & A_{26} & A_{66} & B_{16} & B_{26} & B_{66} \\ B_{11} & B_{12} & B_{16} & D_{11} & D_{12} & D_{16} \\ B_{12} & B_{22} & B_{26} & D_{12} & D_{22} & D_{26} \\ B_{16} & B_{26} & B_{66} & D_{16} & D_{26} & D_{66} \end{bmatrix} \begin{Bmatrix} \varepsilon_\xi^0 \\ \varepsilon_\eta^0 \\ \gamma_{\xi\eta}^0 \\ \kappa_\xi \\ \kappa_\eta \\ \chi_{\xi\eta} \end{Bmatrix} \tag{2}$$

$$\text{where} \quad \begin{Bmatrix} \widehat{N}_\xi \\ \widehat{N}_\eta \\ \widehat{N}_{\xi\eta} \\ \widehat{M}_\xi \\ \widehat{M}_\eta \\ \widehat{M}_{\xi\eta} \end{Bmatrix} = \begin{Bmatrix} N_\xi \\ N_\eta \\ N_{\xi\eta} \\ M_\xi \\ M_\eta \\ M_{\xi\eta} \end{Bmatrix} + \begin{Bmatrix} N_\xi^t \\ N_\eta^t \\ N_{\xi\eta}^t \\ M_\xi^t \\ M_\eta^t \\ M_{\xi\eta}^t \end{Bmatrix} + \begin{Bmatrix} N_\xi^h \\ N_\eta^h \\ N_{\xi\eta}^h \\ M_\xi^h \\ M_\eta^h \\ M_{\xi\eta}^h \end{Bmatrix} \tag{3}$$

are the total laminate generalised stresses, including the contributions of mechanical loading, $\{N\}$ and $\{M\}$, thermal loading, $\{N^t\}$
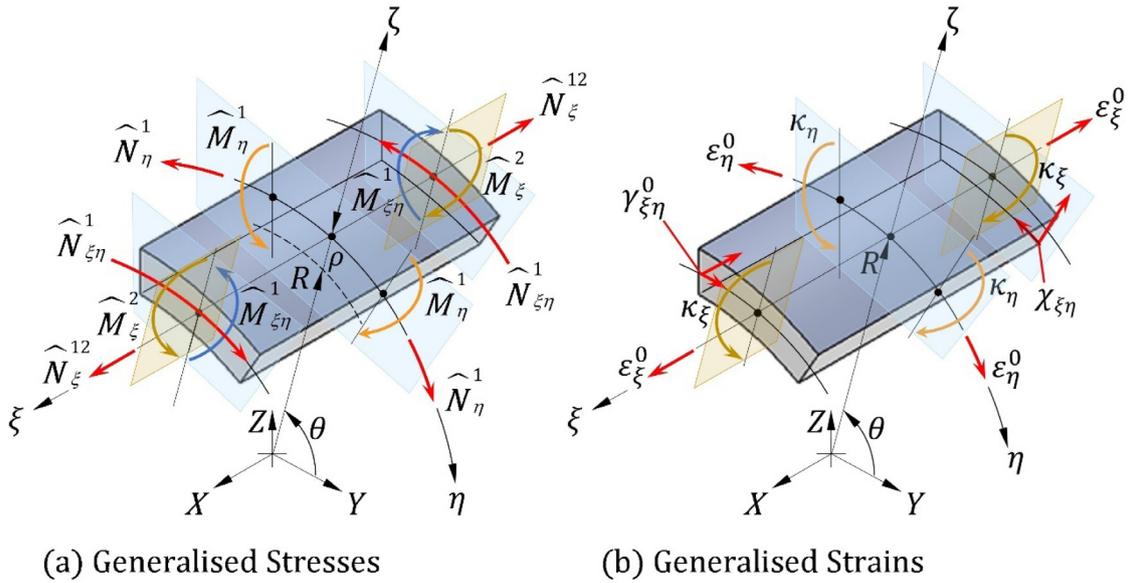
Fig. 4. (a). Generalised stresses where the superscripts, ^{1} and ^{2} refer to the Parts 1 and 2 load cases. (b). Generalised strains appear as they typically occur within the tube under loading.

and $\{M^t\}$, and hydro loading, $\{N^h\}$ and $\{M^h\}$; and $[A]$, $[B]$ and $[D]$ are submatrices of the laminate stiffness. These are all defined in their conventional sense as in CLT [1]. In conjunction with CLT, the tube is considered as a cylindrical shell and the theory of thin elastic shells [12] gives a reasonable approximation when the tube is sufficiently thin, typically as $t < R/10$ [11].

Visualisation of the generalised stresses are shown in Fig. 4a in relation to Parts 1 and 2 loading. Likewise, the generalised strains are indicated in Fig. 4b for the tube under combined loading.

For a given tube, the laminate generalised strains vary around the circumference (θ) of the cross-section in general. However, relationships (1)–(3) hold for any θ. Given the rotational axisymmetry of the tube, laminate stiffness matrices $[A]$, $[B]$ and $[D]$ remain constant at any θ.

The problem will be analysed through three separate load cases as described in Section 3.2 depending on the nature of the distribution of the generalised strains over the tube. In the first load case (Part 1) which involves a temperature change ΔT, moisture absorption Δm, an internal/external pressure q, an axial force P and a torque T_X, the generalised strains generated by these loads are uniform throughout the tube. The second load case (Part 2) consists of bending moments T_Y and T_Z leading to a pure bending problem in which the generalised strains remain constant along the length of the tube but vary linearly in the Y-Z plane as a cross-section of the tube, due to the plane section assumption used. Transverse shear forces Q_Y and Q_Z form the third load case (Part 3) in which the generalise strains vary along the axis of the tube due to the bending moments generated by the shear forces as well as over the cross-section of the tube. Because of this variation, it is necessary to isolate the effect of shear forces and that of the induced moments by selecting the location of the cross-section carefully such that the analysis is conducted on the cross-section where the bending moments happen to vanish. The shear forces will result in only membrane shear force along the circumference in a certain way as addressed in Section 4.3.

4. Determination of the ply stresses within the annular laminated tube

The laminate generalised strains as functions of the global loads (Parts 1–3) are determined and combined by superposition within this section. Ultimately, these strains are used to calculate ply stresses that are required for a failure analysis.

4.1. Part 1 – Laminate deformations due to temperature change, ΔT, moisture absorption, Δm, internal/external pressure, q, axial force, P, and torque, T_X

The objective of this section is to obtain the generalised laminate strains (ε_ξ^0, ε_η^0, $\gamma_{\xi\eta}^0$, κ_ξ, κ_η and $\chi_{\xi\eta}$) as a result of a temperature change, ΔT, a moisture absorption, Δm, an internal/external pressure, q, an axial force, P, and a torque, T_X. To achieve this, it is helpful to associate the laminate generalised strains with the relevant global deformations, ε_X, ϕ_X and ρ to establish the relationship between the global loads and the global deformations.

The deformation kinematics requires

$$\varepsilon_\xi^0 = \varepsilon_X$$
$$\varepsilon_\eta^0 = \rho/R \tag{4a}$$
$$\gamma_{\xi\eta}^0 = -R\phi_X$$

where ε_X, ρ and ϕ_X are three of the global deformations of the tube involved in this load case. Due to the rotational axisymmetry of the structure as well as the loads involved, the axis of the tube is expected to remain straight. As nothing varies in the axial direction, each generator of the cylindrical surface remains straight. Therefore, one has

$$\kappa_\xi = 0 \tag{4b}$$

When dealing with shells, there are various shell theories, each having subtle differences. The one employed in the FEM (Section 5.3) was claimed to be 'consistent' based on the Koiter–Sanders shell theory [13] but that theory misses some obvious terms from the changes of shell curvature, although these terms are usually insignificant if the shell is thin. For cylindrical shells, Vlasov shell theory [14] tends to be more reasonable, as it leads to the following kinematic relationships which are simply geometric observations one can make.

$$\kappa_\eta = -\varepsilon_\eta^0/R = -\rho/R^2$$
$$\chi_{\xi\eta} = \gamma_{\xi\eta}^0/R = -\phi_X. \tag{4c}$$

The curvature changes given in (4c) are not available in FEM, which reveals its insufficiency at least from this perspective.

$$
\begin{Bmatrix} P \\ q \\ T_X \end{Bmatrix} + \begin{Bmatrix} 2\pi R N_\xi^t \\ N_\eta^t / R \\ 2\pi R \left(R N_{\xi\eta}^t + M_{\xi\eta}^t \right) \end{Bmatrix} \Delta T + \begin{Bmatrix} 2\pi R N_\xi^h \\ N_\eta^h / R \\ 2\pi R \left(R N_{\xi\eta}^h + M_{\xi\eta}^h \right) \end{Bmatrix} \Delta m
$$
$$
= \begin{bmatrix} 2\pi R A_{11} & 2\pi R \left(A_{12}/R - B_{12}/R^2 \right) & -2\pi R \left(R A_{16} + B_{16} \right) \\ A_{12}/R & A_{22}/R^2 - B_{22}/R^3 & -\left(R A_{26} + B_{26} \right)/R \\ -2\pi R \left(R A_{16} + B_{16} \right) & 2\pi R \left(-\left(R A_{26} + B_{26} \right)/R + \left(R B_{26} + D_{26} \right)/R^2 \right) & 2\pi R \left(R \left(R A_{66} + B_{66} \right) + \left(R B_{66} + D_{66} \right) \right) \end{bmatrix} \begin{Bmatrix} \varepsilon_X \\ \rho \\ \phi_X \end{Bmatrix} \tag{6}
$$

Box I.

On the other hand, the following generalised stresses are related directly to the loads applied to the tube as equilibrium conditions.

$$N_\xi = P/2\pi R$$

$$N_\eta = qR \tag{5}$$

$$R N_{\xi\eta} + M_{\xi\eta} = -T_X/2\pi R$$

where the first two are identical to the cylindrical pressure vessel analysis in MoM and the third is apparently the moment equilibrium about the axis of the tube, specifically, the X axis.

Incorporating the relationships in (4) and (5) above, the generalised stress–strain relationship (2) can be manipulated and reduced to (see Box I) where the three global deformations can be obtained by inversing the matrix on the right-hand side of (6) expressing them in terms of the loads. Detailed derivations for (6) have been provided in the Appendix which are very much in line with the manipulations as employed in the work by Li [15]. Substituting these global deformations into (4), all the generalised strains can be obtained for this load case.

4.2. Part 2 – Laminate deformations due to the loads of bending moments T_Y and T_Z

The deformation of the tube can be described through the angle of rotations (per unit length) of the cross-section ϕ_Y and ϕ_Z corresponding to the applied bending moments T_Y and T_Z. In this load case, the terms corresponding to the hygrothermal effects will not play any part as they have been considered within Section 4.1. According to the plane section assumption, the axial strain on the reference surface of the laminate (taken as the mid-surface) at circumferential location θ can be obtained as

$$\varepsilon_\xi = \varepsilon_X = \phi_Y R \sin\theta - \phi_Z R \cos\theta. \tag{7}$$

The laminate curvature κ_ξ at θ is the rotation per unit length of the cross-section about the axis perpendicular to direction θ, which can be expressed in terms of ε_ξ^0 as

$$\kappa_\xi = \varepsilon_\xi^0 / R \tag{8a}$$

As in the previous load case, one has the following kinematic relationship according to Vlasov shell theory.

$$\chi_{\xi\eta} = \gamma_{\xi\eta}^0 / R \tag{8b}$$

As there is no overall twisting, the only twisting results from the in-plane shear. As it is pure bending, it is expected that the shape of the cross-section will not be subjected to significant change after deformation. Thus, a reasonable approximation is

$$\kappa_\eta = 0 \tag{8c}$$

In absence of internal/external pressure as in the current load case, it is expected that

$$N_\eta = 0 \tag{9a}$$

is an acceptable approximation. Similarly, without applied torque, the following can be taken as a useful approximation

$$N_{\xi\eta} + M_{\xi\eta}/R = 0 \tag{9b}$$

The kinematic relationships in (8) can be employed. After necessary manipulations, the generalised stress–strain relationship (2) reduces to

$$
\begin{Bmatrix} R N_\xi + M_\xi \\ N_\eta \\ N_{\xi\eta} + M_{\xi\eta}/R \\ M_\eta \end{Bmatrix}
$$
$$
= \frac{1}{R} \begin{bmatrix} R^2 A_{11} + 2R B_{11} + D_{11} & R \left(R A_{12} + B_{12} \right) & R^2 A_{16} + 2R B_{16} + D_{16} \\ R A_{12} + B_{12} & R A_{22} & R A_{26} + B_{26} \\ R^2 A_{16} + 2R B_{16} + D_{16} & R \left(R A_{26} + B_{26} \right) & R^2 A_{66} + 2R B_{66} + D_{66} \\ R B_{12} + D_{12} & R B_{22} & R B_{26} + D_{26} \end{bmatrix}
$$
$$
\times \begin{Bmatrix} \varepsilon_\xi^0 \\ \varepsilon_\eta^0 \\ \gamma_{\xi\eta}^0 \end{Bmatrix}. \tag{10}
$$

Given approximate equilibrium relationships (9), the 2nd and 3rd rows of (10) lead to

$$\begin{Bmatrix} \varepsilon_\eta^0 \\ \gamma_{\xi\eta}^0 \end{Bmatrix} = \{\Gamma\} \varepsilon_\xi^0 \tag{11}$$

where

$$\{\Gamma\} = \begin{Bmatrix} \Gamma_1 \\ \Gamma_2 \end{Bmatrix} = - \begin{bmatrix} R A_{22} & R A_{26} + B_{26} \\ R \left(R A_{26} + B_{26} \right) & R^2 A_{66} + 2R B_{66} + D_{66} \end{bmatrix}^{-1}$$
$$\times \begin{Bmatrix} R A_{12} + B_{12} \\ R^2 A_{16} + 2R B_{16} + D_{16} \end{Bmatrix}. \tag{12}$$

Thus, the remaining two rows can be re-written into

$$\begin{Bmatrix} R N_\xi + M_\xi \\ M_\eta \end{Bmatrix} = \frac{1}{R} \left(\begin{Bmatrix} R^2 A_{11} + 2 B_{11} R + D_{11} \\ R B_{12} + D_{12} \end{Bmatrix} \right.$$
$$\left. + \begin{bmatrix} R \left(R A_{12} + B_{12} \right) & R^2 A_{16} + 2R B_{16} + D_{16} \\ R B_{22} & R B_{26} + D_{26} \end{bmatrix} \{\Gamma\} \right) \varepsilon_\xi^0. \tag{13}$$

The procedure for the derivation of (10) and further manipulations to obtain (13) has been briefly outlined in Appendix. From the equilibrium consideration, the applied bending moment can be expressed in terms of the resultant moments of the generalised stresses along the

circumference of the tube as follows

$$T_Y = \oint N_\xi R \sin \theta \, ds + \oint M_\xi \sin \theta \, ds = R \oint \left(N_\xi R + M_\xi \right) \sin \theta \, d\theta$$

$$T_Z = - \oint N_\xi R \cos \theta \, ds - \oint M_\xi \cos \theta \, ds = -R \oint \left(N_\xi R + M_\xi \right) \cos \theta \, d\theta$$

$$(14)$$

where curvilinear integrations are along the closed path of the reference surface of the laminated tube over its cross-section. Additionally, the minus signs involved are to keep consistency between the right-hand rule sign convention for bending moments in the X–Y–Z coordinate system and the sign convention of the generalised stresses in the $\xi - \eta - \zeta$ coordinate system according to CLT.

The 1st row of (13) can be substituted into (14). Given (7), the bending moments (14) can be expressed as

$$T_Y = \frac{1}{\pi} K \phi_Y \oint \sin^2 \theta \, d\theta = K \phi_Y$$

$$T_Z = \frac{1}{\pi} K \phi_Z \oint \cos^2 \theta \, d\theta = K \phi_Z$$

$$(15)$$

where

where $K = \pi R \left(R^2 A_{11} + 2 B_{11} R + D_{11} \right.$

$$\left. + \left[R \left(R A_{12} + B_{12} \right) \quad R^2 A_{16} + 2 R B_{16} + D_{16} \right] \{ \Gamma \} \right) \quad (16)$$

is the bending rigidity of the tube. From (15), the rotations (per unit length) of the tube cross-section due to bending can be obtained as

$$\phi_Y = \frac{1}{K} T_Y$$

$$\phi_Z = \frac{1}{K} T_Z. \quad (17)$$

Having obtained ϕ_Y and ϕ_Z from the applied bending moments T_Y and T_Z as in (17), all generalised strains can be obtained from (7), (11) and (8) for this load case.

4.3. Part 3 – Laminate deformations due to the loads Q_Y and Q_Z

Applied shear forces, Q_Y and Q_Z, make contributions to laminate generalised strains (ε_ξ^0, ε_η^0, $\gamma_{\xi\eta}^0$, κ_ξ, κ_η and $\chi_{\xi\eta}$) as the third part of the load. Under this shear loading condition, with all the laminae in the tube being unidirectionally fibre reinforced composite, the structure is 180° rotationally antisymmetric about the X axis [16]. Specifically, after a 180° rotation about the X axis, the loads reverse their sense whilst the structure remains unchanged. Amongst all the internal forces, displacements and strains (generalised or not), the symmetric ones reverse their sense and the antisymmetric ones maintain their sense. If the circumference of the tube is cut into two equal halves at any two positions opposite to each other, the two edges of each half are 180° apart. The antisymmetry requires that the membrane shear forces, $N_{\xi\eta}(\theta)$ and $N_{\xi\eta}(\theta + \pi)$, at both edges of each half along the generator of the tube point to the same direction. However, given the complementary nature of shear forces, $N_{\xi\eta}(\theta)$ and $N_{\xi\eta}(\theta + \pi)$ should be of opposite sense to each other. According to the mean value theorem in calculus [17], there exists a point within each half of the circumference of the tube where $N_{\xi\eta}(\theta)$ vanishes. This location is denoted as θ_0. A segment from this point to an arbitrary location defined by θ will be taken as a free body shown in Fig. 5 to be considered below. The segment will be subjected to $N_{\xi\eta}$ on the side at θ, whilst that on the opposite side where $\theta = \theta_0$, the membrane shear force vanishes as argued above.

Following the consideration of 'shear stress in beams' as a typical topic in MoM, the presence of the membrane shear force $N_{\xi\eta}(\theta)$ in the wall of the tube at θ is balanced by $dB(\theta)$, where $B(\theta)$ is the resultant axial stress due to bending over the cross-section of the segment of the tube under consideration, and $dB(\theta)$ is its increment with respect to dX due to the variation of the axial stress along the axial direction. This variation results from the variation of bending moments induced by shear forces.
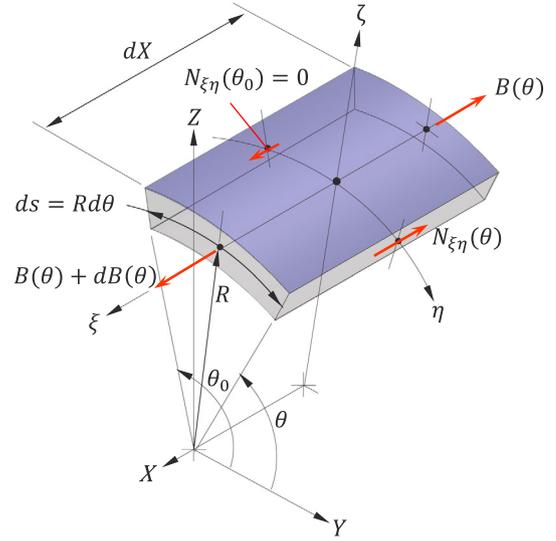
Fig. 5. A segment of the tube for Part 3 loading whereby the global shear forces Q_Y and Q_Z are applied to the tube with resulting membrane force $N_{\xi\eta}(\theta)$.

The equilibrium condition in the axial direction of this free body is

$$N_{\xi\eta}^{(\theta)} dX = -dB(\theta) \qquad \text{or} \qquad N_{\xi\eta}^{(\theta)} = -\frac{dB(\theta)}{dX} \quad (18)$$

where the minus sign is introduced to keep consistency with the sign convention for $N_{\xi\eta}(\theta)$.

In the context of present problem, $B(\theta)$ can be obtained by integrating N_ξ over the cross-section of the segment with N_ξ being expressed in terms of the generalised stress–strain relationship (3) as

$$B(\theta) = \int_\theta^{\theta_0} N_\xi(\theta) \, ds$$

$$= \int_\theta^{\theta_0} \left(A_{11} \varepsilon_\xi^0 + A_{12} \varepsilon_\eta^0 + A_{11} \gamma_{\xi\eta}^0 + B_{11} \kappa_\xi + B_{12} \kappa_\eta + B_{11} \chi_{\xi\eta} \right) ds. \quad (19)$$

The generalised strains involved in (19) are all associated with the bending problem according to MoM. Note that the integral in (19) is taken from θ to θ_0 which specifies the segment as shown in Fig. 5. Using the generalised strains obtained in Section 4.2 for the bending problem, one obtains

$$B(\theta) = \frac{R}{K} \left(\left(R A_{11} + B_{11} \right) + \left[R A_{12} \quad R A_{16} + B_{16} \right] \{ \Gamma \} \right)$$

$$\times \int_\theta^{\theta_0} \left(T_Y \sin \theta - T_Z \cos \theta \right) d\theta \quad (20)$$

$$= H \left(T_Y \left(\cos \theta - \cos \theta_0 \right) + T_Z \left(\sin \theta - \sin \theta_0 \right) \right)$$

where K and Γ are given in (12) and (16), respectively, and

$$H = \frac{R}{K} \left(\left(R A_{11} + B_{11} \right) - \left[R A_{12} \quad R A_{16} + B_{16} \right] \{ \Gamma \} \right). \quad (21)$$

The procedure for the derivation of (20) has been briefly outlined in Appendix. According to MoM, shear forces are related to the derivatives of the bending moments as

$$\frac{dT_Y}{dX} = Q_Z \quad \& \quad \frac{dT_Z}{dX} = -Q_Y \quad (22)$$

where the minus sign is due to the sign convention that the bending moment follows the right-hand rule and that the shear force is in the direction of corresponding coordinate axis. The membrane shear force in the wall of the tube can be obtained as

$$N_{\xi\eta} = -\frac{dB(\theta)}{dx} = H \left(Q_Y \left(\sin \theta - \sin \theta_0 \right) - Q_Z \left(\cos \theta - \cos \theta_0 \right) \right). \quad (23)$$

It should be noted that θ_0 in (19) has not been determined yet. This can be addressed as follows. If one integrates the component of

$N_{\xi\eta}(\theta)$ projected onto the θ_0 direction over half of the cross-section from $-\pi + \theta_0$ to θ_0, it should produce the component of the resultant of $N_{\xi\eta}(\theta)$ over the half cross-section in this direction as

$$R_{\theta_0} = W \left(\frac{1}{2} \left(Q_Z \sin\theta_0 + Q_Y \cos\theta_0 \right) + \frac{2}{\pi} \left(Q_Z \cos\theta_0 - Q_Y \sin\theta_0 \right) \right) \quad (24)$$

where $W = \pi R H = \pi R^2 \left(\left(R A_{11} + B_{11} \right) + \begin{bmatrix} R A_{12} & R A_{16} + B_{16} \end{bmatrix} \{\Gamma\} \right) / K.$

$$(25)$$

It can be proven that $W = 1$ for homogeneous orthotropic tubes. Numerical results suggest that $W \approx 1$ remains as a reasonable approximation for laminated tubes.

On the other hand, given the rotational antisymmetry, equilibrium of the half tube requires

$$R_{\theta_0} = \frac{1}{2} \left(Q_Z \sin\theta_0 + Q_Y \cos\theta_0 \right). \quad (26)$$

Comparing (24) and (26), under the approximation of $W \approx 1$, one obtains

$$Q_Z \cos\theta_0 - Q_Y \sin\theta_0 \approx 0 \qquad \text{or} \qquad \tan\theta_0 = \frac{\sin\theta_0}{\cos\theta_0} \approx \frac{Q_Z}{Q_Y}. \quad (27)$$

In other words, θ_0 coincides approximately with the direction of resultant shear force. In the case of a single shear force Q_Z, the location is $\theta_0 \approx \pm\pi/2$ where the membrane shear force $N_{\xi\eta}$ vanishes.

In order to obtain the generalised strains in the laminate under loads Q_Y and Q_Z, it seems reasonable to approximate that all changes in curvature vanish, or

$$\kappa_\xi = \kappa_\eta = \chi_{\xi\eta} = 0. \quad (28)$$

In addition, in the absence of bending moments over the cross-section and the internal pressure, the following can be assumed based on the equilibrium considerations.

$$N_\xi + M_\xi / R = 0$$
$$N_\eta = 0. \quad (29)$$

Under conditions (28) and (29), the generalised stress–strain relationship (2) can be manipulated to give the following.

$$\begin{Bmatrix} \varepsilon_\xi^0 \\ \varepsilon_\eta^0 \end{Bmatrix} = - \begin{bmatrix} R A_{11} + B_{11} & R A_{12} + B_{12} \\ A_{12} & A_{22} \end{bmatrix}^{-1} \begin{Bmatrix} R A_{16} + B_{16} \\ A_{26} \end{Bmatrix} \gamma_{\xi\eta}^0 \quad (30a)$$

$$\gamma_{\xi\eta}^0 = \frac{1}{A_{66}} \left(N_{\xi\eta} - \begin{bmatrix} A_{16} & A_{26} \end{bmatrix} \begin{Bmatrix} \varepsilon_\xi^0 \\ \varepsilon_\eta^0 \end{Bmatrix} \right) \quad (30b)$$

where $N_{\xi\eta}$ is related to the applied loads Q_Y and Q_Z as expressed in (23) with θ_0 determined through (27). All generalised strains are thus obtained under this load case, given (28).

4.4. Superposition of the load cases

The laminate generalised strains have been obtained for the three load cases, Parts 1, 2 and 3 in Sections 4.1–4.3. The total generalised strains are obtained as a superposition of these three parts as follows

$$\begin{Bmatrix} \varepsilon_\xi^0 \\ \varepsilon_\eta^0 \\ \gamma_{\xi\eta}^0 \\ \kappa_\xi \\ \kappa_\eta \\ \chi_{\xi\eta} \end{Bmatrix}_{\text{Total}} = \begin{Bmatrix} \varepsilon_\xi^0 \\ \varepsilon_\eta^0 \\ \gamma_{\xi\eta}^0 \\ \kappa_\xi \\ \kappa_\eta \\ \chi_{\xi\eta} \end{Bmatrix}_{\text{Part 1}} + \begin{Bmatrix} \varepsilon_\xi^0 \\ \varepsilon_\eta^0 \\ \gamma_{\xi\eta}^0 \\ \kappa_\xi \\ \kappa_\eta \\ \chi_{\xi\eta} \end{Bmatrix}_{\text{Part 2}} + \begin{Bmatrix} \varepsilon_\xi^0 \\ \varepsilon_\eta^0 \\ \gamma_{\xi\eta}^0 \\ \kappa_\xi \\ \kappa_\eta \\ \chi_{\xi\eta} \end{Bmatrix}_{\text{Part 3}} \quad (31)$$

4.5. Determination of the ply stresses

Once the total laminate generalised strains have been found using (31), the ply strains can be obtained from (1). These need to be transformed from the laminate coordinate system ξ-η-ζ to the laminar principal coordinate system 1–2–3. From the laminar stress–strain relationship as part of CLT, stresses within the laminate can be determined, which completes the conventional CLT analysis [1].

If an appropriate composite failure criterion is employed, such as the Tsai–Wu criterion or the maximum stress criterion, the most critical location over the cross-section of tube can be determined and the failure of the tube at this cross-section can be predicted. After considering all critical cross-sections under all critical loading conditions, a mathematical routine can be employed to optimise the layup of the tube and to minimise the weight of the tube. This forms the basis of the TALON (Tubular Axle Laminate Optimisation Numerator) design methodology, although the failure analysis and the optimisation are not within the scope of this paper.

5. Verification and validation

The tubular analysis set out in Section 4 first is verified against an MoM approach for a homogeneous tube of an isotropic material. Next, an FEM validation is undertaken comprising combined loading cases selected to assess the present analytical approach. It should be noted that, in addition to the obvious difference between the analytical nature of the present solution and numerical nature of the FEM analysis, the theoretical frameworks underlying these two approaches are different, the former being derived from CLT which is based on the Love–Kirchhoff hypothesis, whilst the latter is formulated under the 1st order transverse shear deformable theory based on the Reissner–Mindlin hypothesis. Given the disparity in between, the FEM analysis would serve as an independent means to validate the solution as present in this paper.

5.1. Special case of homogeneous and isotropic materials as 'sanity checks'

The analysis presented in this paper is primarily an extension of the conventional MoM approach from homogeneous and isotropic materials to laminated, fibre reinforced composites. As a 'sanity check', the material in the present analysis is reduced to a homogeneous and isotropic material as a special case. Predictably, all results from MoM have been analytically reproduced exactly. These results can be superposed for a combined loading condition.

5.2. Verifications of various assumptions and approximations introduced in the model

The deformation kinematics and the equilibrium considerations in load case 1 (Part 1) can be considered as precise. However, for load cases 2 and 3 (Parts 2 and 3), various assumptions and approximations on deformation kinematics and the equilibrium conditions have to be made to facilitate the respective formulations, notably (7)–(9) for load case 2 and (27)–(29) for load case 3. None of these are made in FEM. However, all FE cases analysed tend to support them as reasonable approximations. The results from specific cases are shown in Section 5.3.

5.3. Validation using FEM

Given the 'sanity checks' and the verifications described in the previous subsections, the analysis progresses to systematic validation using finite elements (FE) as a different and hence independent approach to the same problem. Commercial FE code, Abaqus/Standard [18], was employed. A typical FE model of the tube employed in this study is shown in Fig. 6, where the constraints applied, in terms of kinematic

$$u_\xi\big|_{RP} = u_\xi\big|_{edge} \quad u_\eta\big|_{RP} = u_\eta\big|_{edge}$$

$$\beta_\xi\big|_{RP} = \beta_\xi\big|_{edge} \quad \beta_\eta\big|_{RP} = \beta_\eta\big|_{edge}$$

$$u_\xi = u_\eta = \beta_\xi = \beta_\eta = 0$$

(a). Constraint   (b). Boundary   (c). Mesh
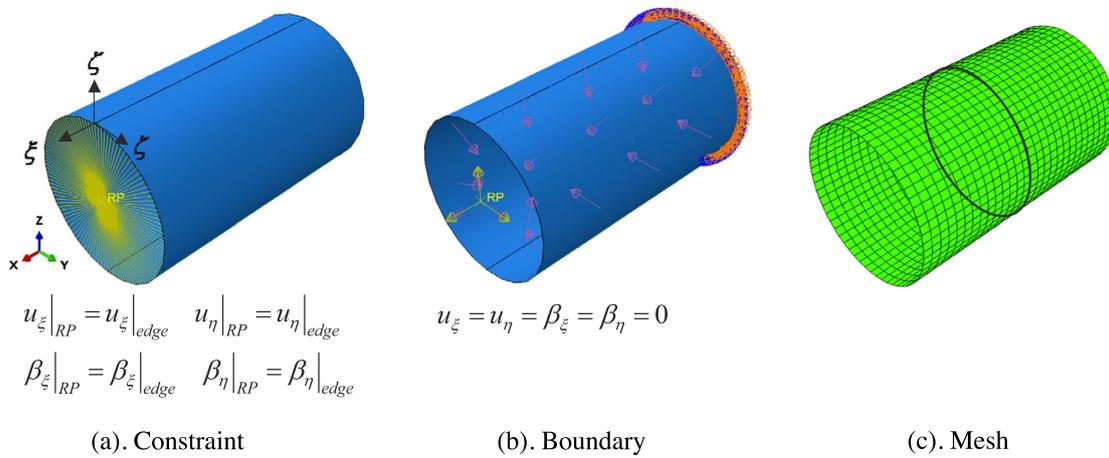
Fig. 6. Typical finite element model of annular tube in validation exercises: (a). Constraint at the loading edge; (b). Boundary conditions at the fixed end; (c). Mesh. Notations 'β' signifies the rotation about the respective axis.

coupling between the reference point (RP) and the loading edge and displacements constraints at the fixed end of the tube, are specified in Fig. 6(a) and (b), respectively. Note that the constraints have been applied in the local (cylindrical) coordinate system, while all the loads but the internal pressure have been prescribed at the RP in the global coordinate system. Shell elements (S8R) were used for modelling thin-walled tubes whilst allowing a laminated composite to be defined. The assumptions of small deformation and small thickness relative of the radius are observed.

Prior to analysing general loading cases and comparing the predictions with respective MoM solutions, the FE model was established in terms of mesh convergence, prescription of boundary conditions, applications of loads, and post-processing of the numerical results. This was achieved by analysing each load case with the material of the tube being defined as homogeneous and isotropic. This exercise has shown that the tube should be sufficiently long to avoid the boundary effects from both ends of the tube. Specifically, in validation cases detailed in Table 1, lengths of the tubes were 100 mm in cases 1 and 3 and 200 mm in case 2. The stresses, generalised stresses, strains and displacements have been read along the central cross-section of the tube marked by black line in Fig. 6(c) where the resultant forces and moments are identical to the desired global loads. As for linearly elastic problems, the underlying basis of the finite element method is the minimum total potential energy (TPE) principle. The convergence of the mesh can be best shown through the convergence of the minimised TPE, $\Pi_{\min}$. Although this is not directly available as an Abaqus output, it can be obtained indirectly according to the minimum TPE principle as being equal to half of the value of the potential of external forces, or negative the value of the total strain energy, ALLSE, which are directly available from Abaqus. The results in Fig. 7 indicate that there are marginal differences between energy values when number of elements exceeds 160. However, in validation exercises, the model meshed with 1680 elements was used to ensure that the subtle variations of stresses are reflected in stress output that was involved in the validation exercises.

Once the FE model was fully established as detailed above, almost perfect agreement was obtained between the FE predictions and the MoM solutions with the largest error well within 1%. As the MoM solutions are all reproduced by the present analysis, the agreement between the FE model and the present analysis was fulfilled when the material is homogeneous and isotropic.

The validation cases are all for laminated composite tubes under a range of combined loads and a set of representative results are listed in Table 1. These cases are introduced intentionally for validation of the present analytical theory [1,19,20]. The agreement serves as a positive endorsement on the present analysis.
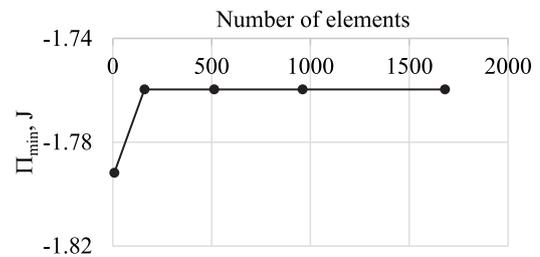
Fig. 7. Mesh convergence study.

Thermal effects have been incorporated into the 2nd validations case. Although the hygro effects can be incorporated in a similar way, due to the lack of relevant material properties, this aspect has not been included in the validation cases considered.

Of note is that although FEM can be employed to analyse the problem addressed within this paper, this does not undermine the present analysis. The analytical nature of this work is inherently more resource-efficient than a commercial FE code. As such, there is no requirement for meshing or other pre- and post-processing routines. Correctly prescribing boundary conditions and applying loads to a FE model is a non-trivial task requiring considerable time, even for a skilled FE user. Most importantly, the present analysis can be incorporated easily into any existing mathematical optimisation routine to provide a comprehensive design tool. This will ease the process of the initial design of laminated composite tubular structures where FEM is less practical for this purpose.

The close agreement between the present analysis and FEM results on the global deformations are evident from Table 1. The laminate generalised strains have been obtained both from the present analysis as given in (31) and FE analysis according to their respective definitions. These are presented and compared in Fig. 8. Graphically, the generalised strain curves appear virtually identical for the 3 validation cases. Exceptions are associated with the curvature changes. In fact, the curvature changes in the longitudinal direction κ_ξ show excellent agreement. Disparities are present in the remaining two curvatures, κ_η and $\chi_{\xi\eta}$. The present analysis predicts constant values for these two curvatures indicting that they are associated primarily with load case 1, see (4c). As indicated in Section 4.1, these curvature changes could not be predicted by FEM due to the insufficiency of the shell theory (Koiter–Sanders) adopted by that method. Rather, the FEM predicted curvature values for κ_η and $\chi_{\xi\eta}$ result from load cases 2 and 3 which the present analysis assumed as either to vanish, (28) and (8c), or be of insignificant value (8b). The magnitude of the FEM predicted values are

Table 1
Validation cases: inputs and results.

		Validation case 1			Validation case 2			Validation case 3		
Input	Composite	Graphite/epoxy [1]			Carbon/epoxy [19]			S-glass/epoxy [20]		
	Layup	$[0°/45°/90°/−45°]_s$			$[0°/45°/0°/−45°/90°]$			$[0°/60°/−60°/0°]$		
	Ply thickness, mm	0.10			0.20			0.25		
	E_1, GPa	207			138			52		
	E_2, GPa	5.0			11.0			19.0		
	G_{12}, GPa	2.6			5.5			6.7		
	ν_{12}	0.25			0.28			0.30		
	α_1, /°C	N/A			$−1 \times 10^{-6}$			8.6×10^{-6}		
	α_2, /°C	N/A			26×10^{-6}			26.4×10^{-6}		
	ΔT, °C	N/A			100			0		
	R, mm	20			69.8			30		
	t, mm	0.8			1.0			1.0		
	q, MPa	2			1			-1		
	P, kN	2			1			1.5		
	Q_Y, kN	1			1.5			2		
	Q_Z, kN	1.5			0.5			1		
	T_X, N m	400			1500			200		
	T_Y, N m	100			500			700		
	T_Z, N m	50			900			150		
		Present analytical	FEM	Error, %	Present analytical	FEM	Error, %	Present analytical	FEM	Error, %
Results	ε_X, $\times 10^{-4}$	0.5194	0.5252	1.11	−2.228	−2.220	0.36	4.988	5.018	0.6
	ϕ_X, $\times 10^{-1}$ m^{-1}	3.613	3.613	0.01	0.3974	0.3967	0.19	1.183	1.184	0.1
	ϕ_Y, $\times 10^{-2}$ m^{-1}	6.830	6.829	0.02	0.6627	0.6614	0.19	23.69	23.69	0.0
	ϕ_Z, $\times 10^{-2}$ m^{-1}	3.415	3.358	1.71	1.193	1.167	2.21	5.076	5.000	1.5
	ρ, $\times 10^{-5}$ m^{-1}	1.198	1.197	0.03	12.30	12.49	1.52	−3.563	−3.570	0.2
	θ_0, °	56.31	56.32	1.21	18.43	18.39	0.23	26.57	26.59	0.1

indeed insignificant and tend to fluctuate around 0. Once incorporated into (1) to produce laminar strains, their contributions are negligible.

Excellent agreement between the present analysis and the FEM results are further demonstrated through the predicted ply stresses. As the stresses vary through the thickness, only those on the inner and outer most surfaces of the tube are plotted in Fig. 9 for comparisons. A slight discrepancy in the stress in the direction transverse to fibres, σ_2, is noted. This is most pronounced in the 3rd validation case (Figs. 9e and 9f). The discrepancy is a further manifestation of the curvature effects as noted for Fig. 8. The strain resulting from the curvature change between approaches is, in fact, hardly noticeable. However, when evaluating stresses, both direct strains are involved and, in this particular case, these two strains happen to be in opposite sense. The discrepancy in the stress is amplified to the magnitude as shown in Figs. 9e and 9f because of this coincidence.

6. Conclusions

This work presents a novel analysis method using classic laminate theory (CLT) in concert with a mechanics of materials (MoM) approach for determining the ply stresses within a radially laminated beam/shaft

of annular cross-section under combined loading conditions. The efficiency of the solution lends itself to adoption as a design tool for hollow composite shafts comprising isotropic and anisotropic materials. Using this method iteratively with a full FEM analysis enables rapid optimisation of the ply stack for the loaded shaft component.

The analysis proceeds with the definition of the global loads applied at the cross-section: hygrothermal, axial, bending, torsional, transverse shear and pressure loads. Importantly, any combination is permissible. The loads produce deformations at the cross-section when observing the plane section assumption. These global deformations are related to those at laminate level along with the laminate stresses through classic laminate theory (CLT). Midplane strains in the laminate are calculated using CLT and expressed in terms of the global forces. Using these midplane strains within the Kirchhoff–Love hypothesis allows calculation of the ply level strains, and stresses around the circumference of the annular section. Use of a laminate failure criteria, such as the Tsai–Wu criterion, in conjunction with the ply stresses would permit an optimised laminate to be specified.

As a basic verification, the present stress analysis of laminated composites tubes is applied to tubes of homogeneous and isotropic materials using MoM formulae. The numerical results were, predictably,
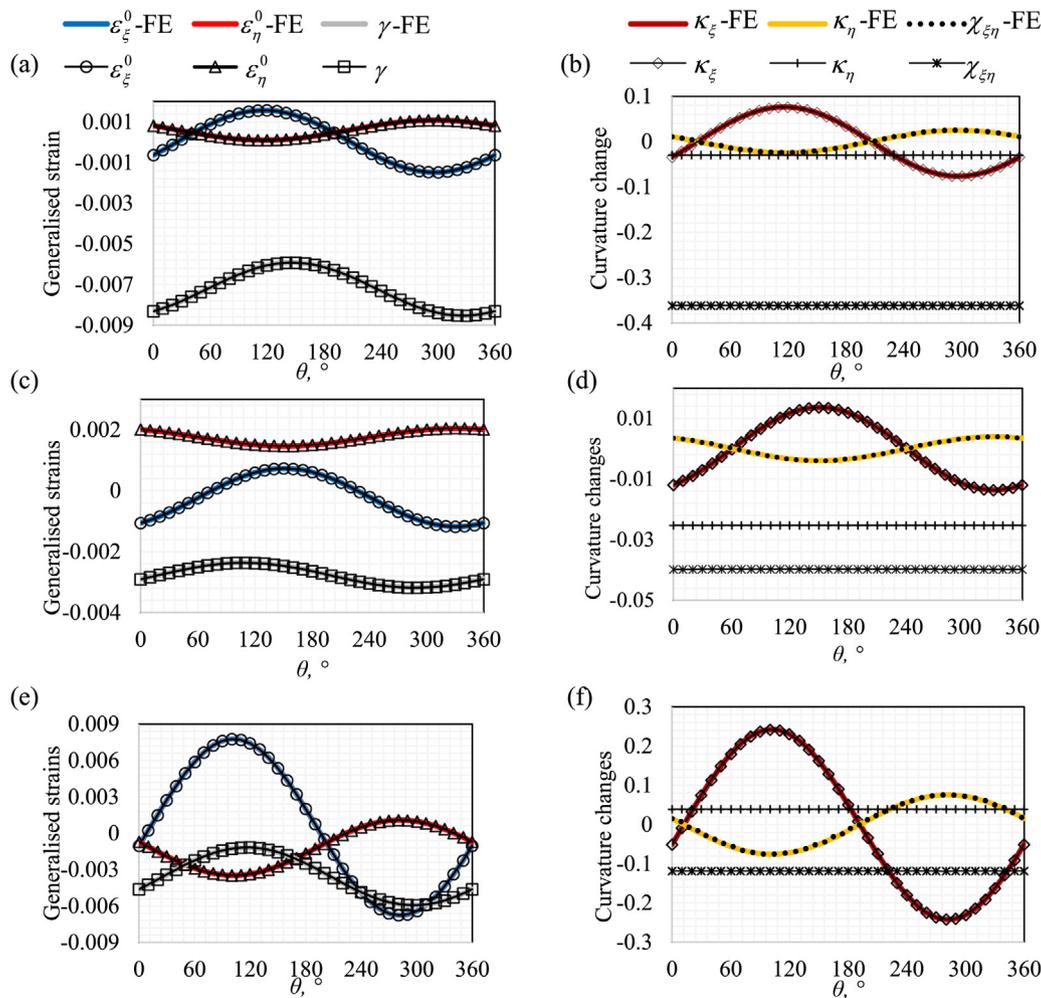
Fig. 8. Comparisons of generalised strains predicted from the present analysis and FEM (a) & (b). Validation case 1. (c) & (d). Validation case 2. (e) & (f). Validation case 3.

identical. As a more serious verification, all assumptions and approximations introduced in the formulation of the present analysis have been examined under individual loads and have been exactly satisfied. The assumptions and approximations are also supported by the FEA results.

Next, a number of validation cases are produced to compare corresponding FEM solutions (Abaqus/Standard) to the present analytical solution. The global displacements were within 2%. The agreements in the distributions of generalised strains and stresses on the outer and inner surfaces are convincing. Minor differences between the present analytical solution and the FEM results are apparent in the circumferential and twisting curvatures. The present analytical solution makes logical assumptions regarding these curvatures while the FEM is disadvantaged by limitations of its underlying shell theory (Koiter–Sanders).

CRediT authorship contribution statement

Shuguang Li: Writing – review & editing, Writing – original draft, Methodology, Formal analysis, Conceptualization. **Michael S. Johnson:** Writing – review & editing, Writing – original draft, Visualization, Supervision, Conceptualization. **Elena Sitnikova:** Validation, Formal analysis. **Richard Evans:** Validation, Formal analysis. **Preetum J. Mistry:** Writing – review & editing.

Declaration of competing interest

The authors declare that they have no known competing financial interests or personal relationships that could have appeared to influence the work reported in this paper.

Data availability

The data that has been used is confidential.

Acknowledgements

Appendix

Eqs. (4a)–(4c) can be summarised into the following kinematic equation which can be employed to express laminate generalised strains
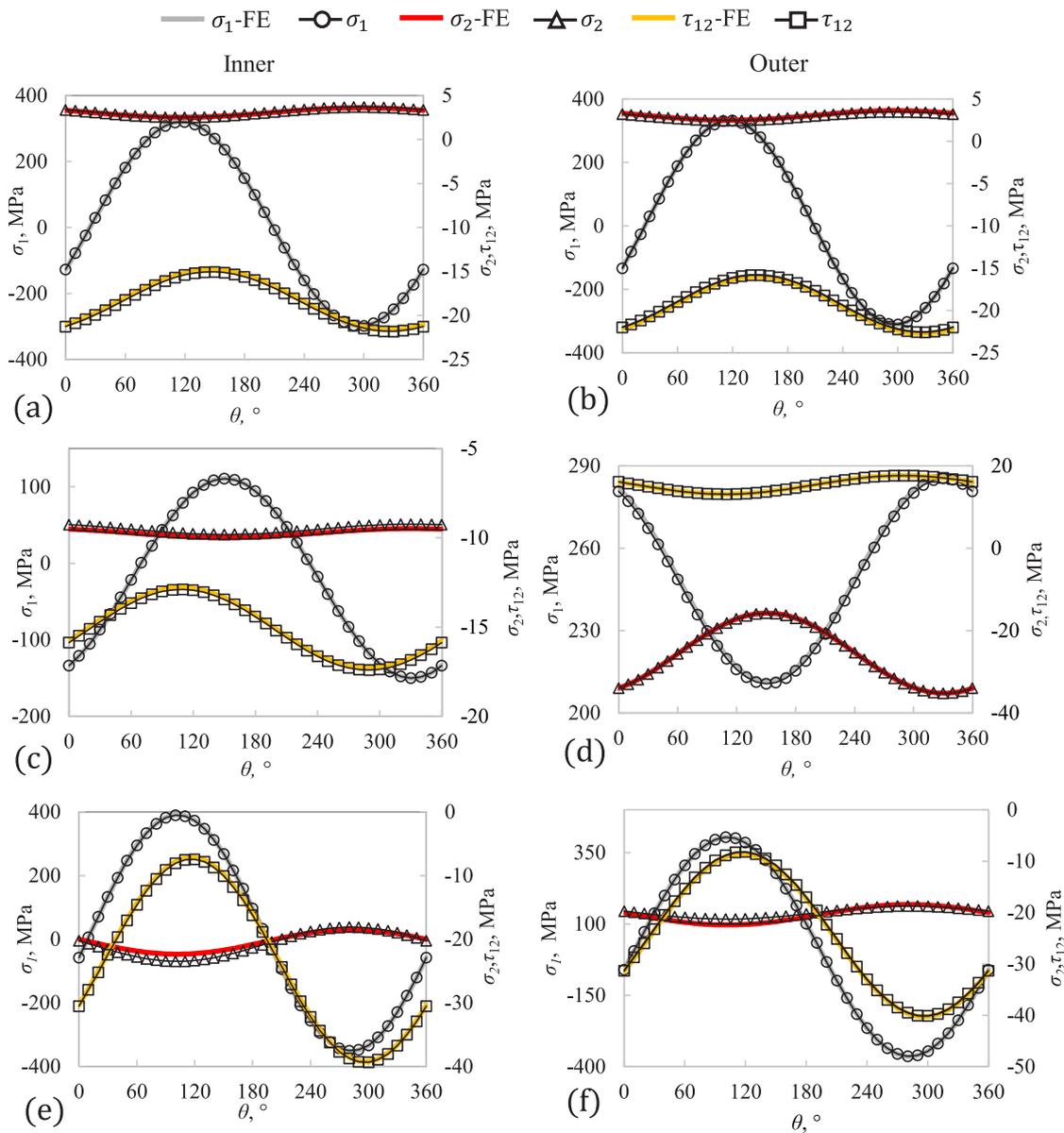
Fig. 9. Ply stresses on the inner most and outer most surfaces of the tubes predicted from the present analysis and FEM (a) & (b). Validation case 1. (c) & (d). Validation case 2. (e) & (f). Validation case 3.

in terms of global deformations for loading case Part 1:

$$\begin{Bmatrix} \varepsilon_\xi^0 \\ \varepsilon_\eta^0 \\ \gamma_{\xi\eta}^0 \\ \kappa_\xi \\ \kappa_\eta \\ \chi_{\xi\eta} \end{Bmatrix} = \begin{Bmatrix} \varepsilon_X \\ \rho/R \\ -R\phi_X \\ 0 \\ -\rho/R^2 \\ -\phi_X \end{Bmatrix} \quad \text{(A.1)}$$

The total laminate generalised stresses, including the contributions of mechanical loading, $\{N\}$ and $\{M\}$, thermal loading, $\{N^t\}$ and $\{M^t\}$, and hydro loading, $\{N^h\}$ and $\{M^h\}$, have been given in (3). Using the relationship between the laminate generalised stresses and global loads

$$N_\xi = P/2\pi R$$

$$N_\eta = qR \quad \text{(A.2)}$$

$$RN_{\xi\eta} + M_{\xi\eta} = -T_X/2\pi R$$

the transformed laminate generalised stresses are as follows, expressed in terms of global loads as far as possible, which are called transformed because the membrane shear force and twisting moment have been combined to be related to the torque applied. Following the scheme of matrix manipulations as employed in the work by Li [15], the generalised stress–strain relationship (3) leads to (see Box II).

Using the kinematic equation to express laminate generalised strains in terms of global deformations: (see Box III).

Absorbing various coefficients to the global deformations, such as $1/R$, $-R$, etc. into the corresponding columns of the coefficient matrix (see Box IV).

Combining the 2nd and 5th rows because of the common factor ρ and similarly the 3rd and 6th rows because of the common factor ϕ_X: (see Box V).

Partition the above matrix equation into two parts: (see Box VI).

Multiplying the 1st and 3rd equations of (A.8) by $2\pi R$, 2nd by $1/R$, one obtains the relationship between the global loads and global deformations as given in (6).

$$\Psi = \left\{ \begin{array}{c} P/2\pi R \\ qR \\ T_X/2\pi R \\ M_\xi \\ M_\eta \end{array} \right\} + \left\{ \begin{array}{c} N_\xi^t \\ N_\eta^t \\ \left(RN_{\xi\eta}^t + M_{\xi\eta}^t\right) \\ M_\xi^t \\ M_\eta^t \end{array} \right\} \Delta T + \left\{ \begin{array}{c} N_\xi^h \\ N_\eta^h \\ \left(RN_{\xi\eta}^h + M_{\xi\eta}^h\right) \\ M_\xi^h \\ M_\eta^h \end{array} \right\} \Delta m$$

$$= \begin{bmatrix} A_{11} & A_{12} & A_{16} & B_{11} & B_{12} & B_{16} \\ A_{12} & A_{22} & A_{26} & B_{12} & B_{22} & B_{26} \\ -(RA_{16}+B_{16}) & -(RA_{26}+B_{26}) & -(RA_{66}+B_{66}) & -(RB_{16}+D_{16}) & -(RB_{26}+D_{26}) & -(RB_{66}+D_{66}) \\ B_{11} & B_{12} & B_{16} & D_{11} & D_{12} & D_{16} \\ B_{12} & B_{22} & B_{26} & D_{12} & D_{22} & D_{26} \end{bmatrix} \left\{ \begin{array}{c} \varepsilon_\xi^0 \\ \varepsilon_\eta^0 \\ \gamma_{\xi\eta}^0 \\ \kappa_\xi \\ \kappa_\eta \\ \chi_{\xi\eta} \end{array} \right\} \tag{A.3}$$

Box II.

$$\psi = \begin{bmatrix} A_{11} & A_{12} & A_{16} & B_{11} & B_{12} & B_{16} \\ A_{12} & A_{22} & A_{26} & B_{12} & B_{22} & B_{26} \\ -(RA_{16}+B_{16}) & -(RA_{26}+B_{26}) & -(RA_{66}+B_{66}) & -(RB_{16}+D_{16}) & -(RB_{26}+D_{26}) & -(RB_{66}+D_{66}) \\ B_{11} & B_{12} & B_{16} & D_{11} & D_{12} & D_{16} \\ B_{12} & B_{22} & B_{26} & D_{12} & D_{22} & D_{26} \end{bmatrix} \left\{ \begin{array}{c} \varepsilon_X \\ \rho/R \\ -R\phi_X \\ 0 \\ -\rho/R^2 \\ -\phi_X \end{array} \right\} \tag{A.4}$$

Box III.

$$\Psi = \begin{bmatrix} A_{11} & A_{12}/R & -RA_{16} & B_{11} & -B_{12}/R^2 & -B_{16} \\ A_{12} & A_{22}/R & -RA_{26} & B_{12} & -B_{22}/R^2 & -B_{26} \\ -(RA_{16}+B_{16}) & -(RA_{26}+B_{26})/R & +R(RA_{66}+B_{66}) & -(RB_{16}+D_{16}) & +(RB_{26}+D_{26})/R^2 & +(RB_{66}+D_{66}) \\ B_{11} & B_{12}/R & -RB_{16} & D_{11} & -D_{12}/R^2 & -D_{16} \\ B_{12} & B_{22}/R & -RB_{26} & D_{12} & -D_{22}/R^2 & -D_{26} \end{bmatrix} \left\{ \begin{array}{c} \varepsilon_X \\ \rho \\ \phi_X \\ 0 \\ \rho \\ \phi_X \end{array} \right\} \tag{A.5}$$

Box IV.

$$\Psi = \begin{bmatrix} A_{11} & A_{12}/R - B_{12}R^2 & -RA_{16} - B_{16} \\ A_{12} & A_{22}/R - B_{22}R^2 & -RA_{26} - B_{26} \\ -(RA_{16}+B_{16}) & -(RA_{26}+B_{26})/R + (RB_{26}+D_{26})R^2 & R(RA_{66}+B_{66}) + (RB_{66}+D_{66}) \\ B_{11} & B_{12}/R - D_{12}/R^2 & -RB_{16} - D_{16} \\ B_{12} & B_{22}/R - D_{22}/R^2 & -RB_{26} - D_{26} \end{bmatrix} \left\{ \begin{array}{c} \varepsilon_X \\ \rho \\ \phi_X \end{array} \right\} \tag{A.6}$$

Box V.

Similarly, for loading case Part 2, the laminate generalised stress–strain relationship (2) is manipulated using the kinematic relationship (8) for this loading case before relationship (13) is obtained. Making use of known laminate generalised stresses as given (9), the 2nd and

$$
\begin{Bmatrix} P/2\pi R \\ qR \\ T_X/2\pi R \end{Bmatrix} + \begin{Bmatrix} N_\xi^t \\ N_\eta^t \\ RN_{\xi\eta}^t + M_{\xi\eta}^t \end{Bmatrix} \Delta T + \begin{Bmatrix} N_\xi^h \\ N_\eta^h \\ RN_{\xi\eta}^h + M_{\xi\eta}^h \end{Bmatrix} \Delta m
$$

$$
= \begin{bmatrix} A_{11} & A_{12}/R - B_{12}/R^2 & -RA_{16} - B_{16} \\ A_{12} & A_{22}/R - B_{22}/R^2 & -RA_{26} - B_{26} \\ -\left(RA_{16} + B_{16}\right) & -\left(RA_{26} + B_{26}\right)/R + \left(RB_{26} + D_{26}\right)R^2 & R\left(RA_{66} + B_{66}\right) + \left(RB_{66} + D_{66}\right) \end{bmatrix} \begin{Bmatrix} \varepsilon_X \\ \rho \\ \phi_X \end{Bmatrix} \tag{A.7}
$$

$$
\begin{Bmatrix} M_\xi \\ M_\eta \end{Bmatrix} + \begin{Bmatrix} M_\xi^t \\ M_\eta^t \end{Bmatrix} \Delta T + \begin{Bmatrix} M_\xi^h \\ M_\eta^h \end{Bmatrix} \Delta m = \begin{bmatrix} B_{11} & B_{12}/R - D_{12}/R^2 & -RB_{16} - D_{16} \\ B_{12} & B_{22}/R - D_{22}/R^2 & -RB_{26} - D_{26} \end{bmatrix} \begin{Bmatrix} \varepsilon_X \\ \rho \\ \phi_X \end{Bmatrix} \tag{A.8}
$$

Box VI.

3rd equations of (10) can be rearranged into

$$
\begin{bmatrix} RA_{22} & RA_{26} + B_{26} \\ R\left(RA_{26} + B_{26}\right) & R^2 A_{66} + 2RB_{66} + D_{66} \end{bmatrix} \begin{Bmatrix} \varepsilon_\eta^0 \\ \gamma_{\xi\eta}^0 \end{Bmatrix}
$$

$$
= - \begin{Bmatrix} RA_{12} + B_{12} \\ R^2 A_{16} + 2RB_{16} + D_{16} \end{Bmatrix} \varepsilon_\xi^0 \tag{A.9}
$$

and this can be employed to express laminate generalised strains ε_η^0 and $\gamma_{\xi\eta}^0$ in terms of ε_ξ^0. Integration of (13) relates laminate generalised stresses to the global loads in this loading case, and relationship (7) is employed to express laminate generalised strain ε_ξ^0 in terms of global deformations ϕ_Y and ϕ_Z leading to the relationship between global loads and global deformations in this loading case (15).

Loading case Part 3 is a statically determinate problem in which the membrane shear force is determined by the applied shear loads based on equilibrium considerations alone. Laminate generalised stress–strain relationship (2) has been employed to express the obtained membrane shear force in terms of laminate generalised strains, which are closely associated with the bending problem as loading case Part 2, resembles the relationship between shear and bending in MoM. From (19) and making use of (A.10) above

$$
B(\theta) = \int_\theta^{\theta_0} \left(\left(RA_{11} + B_{11}\right) \varepsilon_\xi^0 + \begin{bmatrix} RA_{12} & RA_{16} + B_{16} \end{bmatrix} \begin{Bmatrix} \varepsilon_\eta^0 \\ \gamma_{\xi\eta}^0 \end{Bmatrix} \right) d\theta
$$

$$
= \left(\left(RA_{11} + B_{11}\right) - \begin{bmatrix} RA_{12} & RA_{16} + B_{16} \end{bmatrix} \right.
$$
$$
\times \begin{bmatrix} RA_{22} & RA_{26} + B_{26} \\ R\left(RA_{26} + B_{26}\right) & R^2 A_{66} + 2RB_{66} + D_{66} \end{bmatrix}^{-1}
$$
$$
\left. \times \begin{Bmatrix} RA_{12} + B_{12} \\ R^2 A_{16} + 2RB_{16} + D_{16} \end{Bmatrix} \right) \int_\theta^{\theta_0} \varepsilon_\xi^0 d\theta \tag{A.10}
$$

$$
= \frac{R}{K} \left(\left(RA_{11} + B_{11}\right) - \begin{bmatrix} RA_{12} & RA_{16} + B_{16} \end{bmatrix} \right.
$$
$$
\times \begin{bmatrix} RA_{22} & RA_{26} + B_{26} \\ R\left(RA_{26} + B_{26}\right) & R^2 A_{66} + 2RB_{66} + D_{66} \end{bmatrix}^{-1}
$$
$$
\left. \times \begin{Bmatrix} RA_{12} + B_{12} \\ R^2 A_{16} + 2RB_{16} + D_{16} \end{Bmatrix} \right) \int_\theta^{\theta_0} \left(T_Y \sin\theta - T_Z \cos\theta \right) d\theta.
$$

References

[1] R.M. Jones, Mechanics of Composite Materials, second ed., Taylor & Francis, Washington, D.C. USA, 1998.

[2] F.C. Campbell, Structural Composite Materials, first ed., ASM International, Materials Park, Ohio, USA, 2010.

[3] S.G. Lekhnitskii, Theory of Elasticity of an Anisotropic Body, Mir Publishers, Moscow, Russia, 1981.

[4] C. Jolicoeur, A. Cardou, Analytical solution for bending of coaxial orthotropic cylinders, J. Eng. Mech. 120 (12) (1994) 2556–2574, http://dx.doi.org/10.1061/(ASCE)0733-9399(1994)120:12(2556).

[5] A.N. Stroh, Dislocations and cracks in anisotropic elasticity, Philos. Mag. J. Theor. Exp. Appl. Phys. 3 (30) (1958) 625–646, http://dx.doi.org/10.1080/14786435808565804.

[6] F. Shadmehri, B. Derisi, S.V. Hoa, On bending stiffness of composite tubes, Compos. Struct. 93 (9) (2011) 2173–2179, http://dx.doi.org/10.1016/j.compstruct.2011.03.002.

[7] N. Silvestre, Non-classical effects in FRP composite tubes, Composites B 40 (8) (2009) 681–697, http://dx.doi.org/10.1016/j.compositesb.2009.07.001.

[8] Y. Huang, J.X. Wu, X.F. Li, L.E. Yang, Higher-order theory for bending and vibration of beams with circular cross section, J. Eng. Math. 80 (1) (2013) 91–104, http://dx.doi.org/10.1007/s10665-013-9620-2.

[9] M. Lezgy-Nazargah, A four-variable global–local shear deformation theory for the analysis of deep curved laminated composite beams, Acta Mech. 231 (4) (2020) 1403–1434, http://dx.doi.org/10.1007/s00707-019-02593-7.

[10] J.M. Gere, S.P. Timoshenko, Mechnics of Materials, third SI Edition ed., Springer-Science+Business Media, B.V. UK, 1991.

[11] R.G. Budynas, J.K. Nisbett, Shigley's Mechanical Engineering Design, nineth ed., McGraw-Hill Higher Education, New York, New York, USA, 2011.

[12] H. Kraus, Thin Elastic Shells: An Introduction to the Theoretical Foundations and the Analysis of Their Static and Dynamic Behaviour, Wiley, New York, USA, 1967.

[13] B. Budiansky, J.L. Sanders, On the 'Best' First-Order Linear Shell Theory, Macmillan, London, UK, 1963.

[14] V.Z. Vlasov, The fundamental differential equations of the general theory of elastic shells, Prikl. Mat. Mekh. 8 (2) (1944) 109–140.

[15] S. Li, Rigidities of one-dimensional laminates of composite materials, J. Eng. Mech. 122 (4) (1996) 371–374, http://dx.doi.org/10.1061/(ASCE)0733-9399(1996)122:4371.

[16] S. Li, E. Sitnikova, Representative Volume Elements and Unit Cells, in: Concepts, Theory, Applications and Implementation, Woodhead Publishing Series in Composites Science and Engineering, Elsevier, Duxford, UK, 2019.

[17] P.K. Sahoo, T. Riedel, Mean Value Theorems and Functional Equations, World Scientific, Singapore, 1998.

[18] Abaqus/Standard, Dassault systèmes simulia corp, 2018, 10 Rue Marcel Dassault, CS 40501 78946 Vélizy-Villacoublay Cedex, France.

[19] P.D. Soden, M.J. Hinton, A.S. Kaddour, Lamina properties, lay-up configurations and loading conditions for a range of fibre-reinforced composite laminates, Compos. Sci. Technol. 58 (7) (1998) 1011–1022, http://dx.doi.org/10.1016/S0266-3538980078-5.

[20] A.S. Kaddour, M.J. Hinton, Input data for test cases used in benchmarking triaxial failure theories of composites, J. Compos. Mater. 46 (19–20) (2012) 2281–2282, http://dx.doi.org/10.1177/0021998312449886.